

Optimal parameters for a fixed imaging time acquisition of quantitative magnetization transfer data

M. Cercignani¹, G. J. Barker², and D. C. Alexander³

¹Neuroimaging Laboratory, Santa Lucia Foundation, Rome, Italy, ²CNS, Department of Neuroimaging, King's College London, Institute of Psychiatry, London, United Kingdom, ³Centre for medical image computing, Department of computer science, UCL, London, United Kingdom

Introduction

Quantitative magnetization transfer (MT) enables the estimation of fundamental quantities such as the relative size of macromolecular pool (F), thought to reflect myelination, by fitting an analytical model to a series of acquisitions obtained with differing degrees of off-resonance irradiation. The choice of the combinations of acquisition parameters which modulate the amount of MT-weighting (sampling points) is known to have a crucial effect on the precision of the estimated quantities (1). We previously addressed the issue of optimising the sampling points (1) using the theory of the Cramer Rao lower bound (CRLB) and the MT signal equation proposed by Ramani et al (2). A more flexible signal equation, which explicitly models the dependency of the MT signal on the repetition time TR and imaging flip angle θ was proposed by Sled and Pike (3). Using this model, we now investigate the best combination of acquisition parameters (including TR; imaging flip angle, θ ; amplitude, ω_1 , and offset frequency, Δ , of the saturation pulses), by means of the set which gives the maximum precision of the estimated MT parameters, under the constraint of fixed total scan time. The optimisation is achieved for a number of sampling points ranging from 10 to 18 using an algorithm of an "evolutionary" type (4), and the optimised schemes are compared using numerical simulations. The best sampling scheme is then used to collect in vivo data, and is compared with data from a uniformly spaced scheme with identical scan time, similar to that originally suggested by Sled and Pike (3), but with a reduced number of sampling points.

Methods

Optimization: The optimisation is based on Sled and Pike's continuous wave (CW) approximation of MT (3), where the signal is expressed as a function of ω_1 , Δ , θ and TR. We aim to optimize N-point sampling schemes, with the same total acquisition time. To this aim, we fix the sum of all TRs: $\sum TR_i = T_{tot}$. The total scan time is assumed to be given by $T_{scan} = N1 \cdot N2 \cdot T_{tot}$, where N1 and N2 are, respectively, the number of in-plane and through-plane phase encoding steps in a 3D gradient echo acquisition. As the parameters associated with the free pool (T_2^A and gM_0) are readily measurable by other techniques, we focus on the macromolecular pool parameters by using a cost function including only the 3 diagonal elements of Fisher's information matrix (1,5) that correspond to RM_0^B , F, T_2^B . The cost function is minimised using the stochastic optimization algorithm SOMA (4).

Numerical Simulations: The 9 optimal schemes (one for each N) are compared by means of 1) their objective function value, and 2) numerical simulations. Synthetic sets are created by solving the coupled Bloch Equations for the system and adding Rician noise in a Monte Carlo fashion (10000 iterations). The signal equation is fitted to these synthetic sets using the Levenberg-Marquardt method. We then compare the results, in terms of precision and accuracy of the estimated parameters, between Ns and at various SNR values.

In Vivo Data: A single healthy subject (female, 30 years old) was scanned twice on a GE 1.5 T system (GE Healthcare, Milwaukee, USA) using a 3D MT-weighted fast spoiled-gradient recalled-echo (SPGR) sequence (TE = 4.2ms, matrix = 256x128, FoV = 24cm, 0.75 rectangular field of view). During the first session, the sampling scheme which resulted the best from numerical simulations was used, while during the second session a more "standard" scheme, with a uniform distribution of 13 sampling points with the same T_{tot} , was used. In addition to the MT data, three 3D SPGRs (TR = 7.7 ms, TE = 2.9ms, flip angle = 5°, 15°, 20°, respectively) were collected in each session, for T1 mapping (6). After image co-registration, R_{Aobs} ($=1/T1$) was estimated on a pixel-by-pixel basis by fitting the theoretical SPGR signal equation to the signal in the non-MT weighted SPGR images, as a function of the flip angle (6). Next, Sled and Pike's equation was fitted to the data to yield maps of F, RM_0^B , T_2^A , T_2^B , and gM_0 . In order to obtain a measure of the uncertainty associated with the MT estimates, Monte Carlo Markov Chain was used to draw many samples from the posterior distribution of each parameter in every voxel. Voxel-wise mean and standard deviation were obtained and used to compute the coefficient of variance (CoV - defined as the standard deviation divided by the mean) for each of the 4 parameters, and expressed in percentage units. The CoVs were compared between acquisitions.

Results

The minimum cost function was found for N=11 (fig 1). Numerical simulations show that for both F and RM_0^B , the N=11 scheme performs better than the others, particularly at low SNR (fig 2). The optimized sampling scheme used for in vivo acquisition was therefore that with N=11 (fig 3). The CoVs for the optimized scheme are consistently lower than those for the standard acquisition. This is particularly evident for RM_0^B , where the improvement is nearly 10-fold (fig 4). Moreover, the CoVs appear much more uniform across the slice for the optimized than for the standard scheme data. For both acquisitions, the largest CoV (greater than 10%) are found for T_2^A .

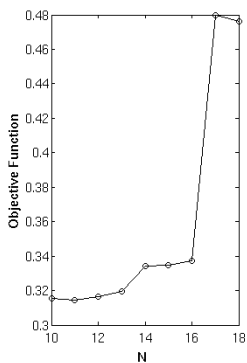


Fig 1. Minimum objective function value as a function of N.

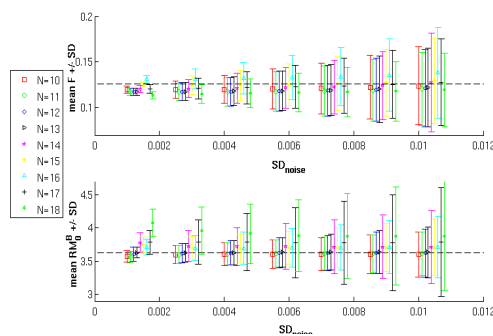


Fig 2. Results of Monte Carlo simulations for F (top), RM_0^B (bottom) for synthetic data. bars indicate the SDs. The dashed black line shows the value used to create the simulation.

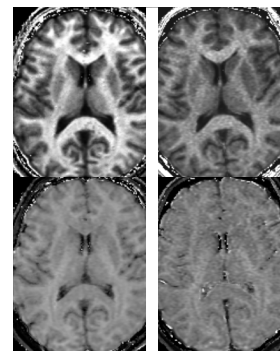


Fig 3. In vivo maps for the optimised scheme (left) and standard scheme (right). Top: F, bottom: T_2^B .

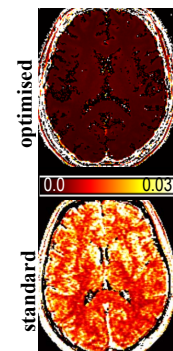


Fig 4. CoV maps for RM_0^B .

Discussion

The experiments suggest that a limited number of sampling points is sufficient to obtain robust MT parameter estimates, and that the available time should be used to include at least one point with long TR. For all N we also found the presence of at least 1 point with either large offset frequency, or very low (near zero) power, thus corresponding to an "unweighted" acquisition. This might reflect the need for an accurate estimation of the signal in the absence of MT saturation in order to fit the remaining parameters accurately (3). In conclusion, the optimisation we presented here confirms and extends previous work. The increased reproducibility provided by the optimised scheme has obvious benefits for research applications, while the potential to reduce scan time while maintaining high data quality may make quantitative MT feasible for clinical applications. The adaptation for the new model that we provide in this paper ties that feasibility to a more accurate model and resolves questions concerning trade-offs between repetition time and sampling density that our earlier optimization procedure left outstanding.

References

1. Cercignani & Alexander, (2006) Magn Reson Med 56:803-810; 2. Ramani et al., (2002) Magn Reson Imaging 20:721-731; 3. Sled & Pike., (2000) J Magn Reson 145:24-36; 4. Zelinska (2004). In: Babu BV, G. O, editors. New optimization techniques in engineering: Springer; 5. Kay (1993) Fundamentals of Statistical Signal Processing: Estimation Theory. Englewood Cliffs, NJ: Prentice Hall; 6. Venkatesan et al, (1998) Magn Reson Med 40:592-602.